Journal of Power Sources 196 (2011) 674–678

Contents lists available at ScienceDirect

Journal of Power Sources

journal homepage: www.elsevier.com/locate/jpowsour

Short communication

Measurement of effective gas diffusion coefficients of catalyst layers of PEM fuel cells with a Loschmidt diffusion cell

Jun Shen[a,*], Jianqin Zhou[a], Nelson G.C. Astrath[a,1], Titichai Navessin[a], Zhong-Sheng (Simon) Liu[a], Chao Lei[a], Jurandir H. Rohling[a,1], Dmitri Bessarabov[b,2], Shanna Knights[c], Siyu Ye[c]

[a] National Research Council of Canada, Institute for Fuel Cell Innovation, 4250 Wesbrook Mall, Vancouver, British Columbia V6T 1W5, Canada
[b] Automotive Fuel Cell Cooperation Corp., 9000 Glenlyon Parkway, Burnaby, British Columbia V5J 5J8, Canada
[c] Ballard Power Systems Inc., 9000 Glenlyon Parkway, Burnaby, British Columbia V5J 5J8, Canada

ARTICLE INFO

Article history:
Received 9 June 2010
Received in revised form 26 July 2010
Accepted 27 July 2010
Available online 4 August 2010

Keywords:
Effective gas diffusion coefficient
Cathode catalyst layer
PEM fuel cells
Knudsen effect
Loschmidt diffusion cell

ABSTRACT

In this work, using an in-house made Loschmidt diffusion cell, we measure the effective coefficient of dry gas (O_2–N_2) diffusion in cathode catalyst layers of PEM fuel cells at 25 °C and 1 atmosphere. The thicknesses of the catalyst layers under investigation are from 6 to 29 μm. Each catalyst layer is deposited on an Al_2O_3 membrane substrate by an automated spray coater. Diffusion signal processing procedure is developed to deduce the effective diffusion coefficient, which is found to be $(1.47 \pm 0.05) \times 10^{-7}$ m^2 s^{-1} for the catalyst layers. Porosity and pore size distribution of the catalyst layers are also measured using Hg porosimetry. The diffusion resistance of the interface between the catalyst layer and the substrate is found to be negligible. The experimental results show that the O_2–N_2 diffusion in the catalyst layers is dominated by the Knudsen effect.

1. Introduction

A cathode catalyst layer (CCL) in a proton exchange membrane (PEM) fuel cell is a porous thin coating with the porosity of 30–60% and pore size distribution from several nanometers to 100 nm. The porosity allows the transport of reactant oxygen into the CCL and the transport of product water vapour out of the CCL. Thus oxygen reduction reaction can happen through the whole depth of the CCL, maximizing current density. Oxygen concentration in air is about 20% and O_2 transports into the CCL mainly through a diffusion process. Consequently, the effective gas diffusion coefficient (EGDC) of the CCL is a very important parameter, which affects the uniformity of oxygen reduction reaction through the whole CCL, the CCL lifetime, and the power density of PEM fuel cells [1]. Therefore, it is in great demand to theoretically calculate this parameter and experimentally measure it.

Theoretically the EGDC of a porous material is correlated to the corresponding gas diffusion coefficient D through empty space, namely the bulk diffusion coefficient, and some statistical parameters of porous microstructure, such as porosity. Some theoretical formulas describing the relation between the EGDC and porosity are available [2–8]. Among the formulas, the Bruggeman's formula [4] is very frequently used for calculating the EGDC of a CCL. But the accuracy of the calculated EGDC is often inadequate and even misleading when pore size distribution of the CCL falls in the region of less than 1 micron, i.e., the Knudsen effect must be considered. In order to quantify the Knudsen effect, a 3D microstructure based method for calculating the EGDC was developed, and a formula relating the EDGC to porosity and Knudsen effect was proposed by Mu et al [2].

Experimental measurement techniques, e.g., gas chromatography, nuclear magnetic resonance (e.g., PFG NMR), and diffusion cell methods, have been developed to determine the EGDCs of porous materials [9–13]. Kramer and co-workers measured the EGDC in carbon paper using electrochemical impedance spectroscopy [14,15]. Zhang et al. [9] used a Wicke–Kallenbach diffusion cell to measure the EGDC of a catalyst monolith washcoat. A closed-tube method with a Loschmidt diffusion cell is considered as one of the most reliable methods to determine binary diffusion coefficients of gases [16–19]. Using a Loschmidt cell, bulk binary diffusion coefficients of O_2–N_2 were precisely measured under the experimental conditions of different temperatures (25–80 °C) and relative

* Corresponding author. Tel.: +1 604 221 3046; fax: +1 604 221 3001,.
E-mail address: Jun.Shen@nrc-cnrc.gc.ca (J. Shen).
[1] Present address: Departamento de Física, Universidade Estadual de Maringá, Avenida Colombo 5790, 87020-900, Maringá, Paraná, Brazil.
[2] Present address: DST Hydrogen Infrastructure Center of Competence (HySA Hydrogen Infrastructure), Faculty of Natural Sciences, Chemical Resource Beneficiation, Private Bag X6001, Potchefstroom 2520, South Africa.

0378-7753/$ – see front matter.
doi:10.1016/j.jpowsour.2010.07.086

humidity values (0–80%) [18]; the EGDCs of gas diffusion layers of PEM fuel cells were also studied at different temperatures [11]. Moreover, the measured EGDC of a porous sample of a stainless steel film with simple straight pores was found to be in good agreement with the result of numerical computation of three-dimensional mass diffusion through the sample [19], exhibiting the usefulness of the Loschmidt cell in studying porous material.

Although the EGDCs of the CCLs in PEM fuel cells are in great demand, and measurement techniques of the EGDC have been developed, little literature can be found on the measured EGDCs of the CCLs of PEM fuel cells. Over the past several years, we have been trying to correlate the CCL microstructure with its EGDC and then its performance. As a part of this effort, we have developed a Loschmidt cell method for measuring the EGDCs of CCLs. In this paper, we present the measurement method first and then the measured EGDC of eight CCL samples, which are different in thickness from 6 to 29 μm but are fabricated with the same composition and the same deposition conditions, allowing us to consider the microstructures of these CCLs to be similar in a statistical sense. Each sample is deposited on an Al_2O_3 membrane substrate. In order to measure the EGDC of eight CCLs, the bulk diffusion coefficient and the EGDC of the substrate have to be measured first. Our measurement indicates that the EGDC is one order of magnitude lower than the Bruggeman formula [4] gives, meaning that the Knudsen effect is dominant and must not be neglected. This result confirms our previous calculations of the EGDCs of CCLs [2].

2. Experimental

2.1. Experimental setup

The in-house made Loschmidt diffusion cell comprised two chambers, separated by a valve (at $z = 0$), as schematically shown in Fig. 1. The chambers were maintained at 25 °C and 1 atmosphere in this work. At the beginning of a measurement, the top chamber was filled with N_2, while the bottom chamber was full of O_2. When the valve opened the binary gas diffusion started, and an optic fibre oxygen sensor located at ($z = Z$) measured the oxygen concentration value in the top chamber. The diffusion coefficient was deduced from the oxygen concentration evolution with time in the top chamber detected by the oxygen sensor. A computer controlled the whole experimental procedure, including gas filling the chambers, signal collection from the oxygen sensor, and temperature maintenance of the cell. The detailed description of the experimental setup and experimental procedure can be found in Refs. [11,18]. In this work, the ball valve in Refs. [11,18] was replaced by a flat one, and $Z = 1.595 \times 10^{-2}$ m.

2.2. Processing of diffusion signals

In this work for the Loschmidt diffusion cell shown in Fig. 1, the O_2–N_2 diffusion coefficient can be attained from the oxygen concentration evolution in the top chamber based on the one-dimensional Fick's second law of diffusion [16,17,20]:

$$\frac{\partial C(z,t)}{\partial t} = D\frac{\partial^2 C(z,t)}{\partial z^2}, \tag{1}$$

with the initial conditions and the impermeable boundary conditions at $z = \pm L/2$:

$$C = C_b \qquad \left(-\frac{L}{2} \le z < 0, \quad t = 0\right), \tag{2}$$

$$C = C_t \qquad \left(0 < z \le +\frac{L}{2}, \quad t = 0\right), \tag{3}$$

$$\left(\frac{\partial C}{\partial z}\right)_{z=\pm L/2} = 0 \qquad (t > 0). \tag{4}$$

$C(z,t)$ is the oxygen concentration, D the diffusion coefficient. L is the length of the Loschmidt cell. C_b and C_t are the concentrations of O_2 at $t = 0$ in bottom and top chambers, respectively. The solution of Eq. (1) is [17–19]

$$C(z,t) = \frac{1}{2}\left[C_b + C_t - (C_b - C_t)\,erf\left(\frac{z}{2\sqrt{Dt}}\right)\right] \qquad (t < 0.1\tau). \tag{5}$$

$erf(x)$ is the error function, and $\tau = L^2/(\pi D)$ is the characteristic diffusion time. Refs. [17,18] exhibit that for a short period $t < 0.1\tau$, Eq. (5) well describes the bulk diffusion (diffusion without any porous sample in the diffusion cell) of a binary gas mixture. The bulk diffusion coefficient D can be deduced by least-square curve fitting Eq. (5) to the curve of oxygen concentration evolution in the top chamber sensed by the oxygen sensor.

In the presence of a porous sample located between $z = 0$ and $z = Z$ in the top chamber in Fig. 1, an equivalent resistance R_{eq} to binary gas diffusion may be introduced [9].

$$R_{eq} = \frac{Z}{D_{eq}A}, \tag{6}$$

where D_{eq} is the equivalent diffusion coefficient of the medium from the $z = 0$ to $z = Z$, and A is the cross-sectional area available to diffusion. In this case, the D in Eq. (5) should be replaced by D_{eq}. The oxygen concentration evolution curve after diffusion through the porous sample can be measured with the oxygen sensor, and the D_{eq} can be deduced with Eq. (5) by the foregoing curve-fitting method. The concept of the equivalent resistance originates from electrical conduction, and sometimes heat conduction analysis adapts the concept. In this method, the object is considered to be comprised of a number of individual resistances, which can be connected to form an overall circuit [9]. In the presence of a porous sample located between $z = 0$ and $z = Z$, the equivalent resistance to gas diffusion is formed by bulk diffusion resistance and porous sample resistance, and they are connected in series.

In the case of a single layer porous sample of thickness l and effective diffusion coefficient D_{eff}, the equivalent resistance can be considered the sum of the bulk diffusion resistance and the diffusion resistance through the porous sample.

$$R_{eq} = \frac{Z}{D_{eq}A} = \frac{Z-l}{DA} + \frac{l}{D_{eff}A}. \tag{7}$$

The D_{eff} can be calculated with

$$D_{eff} = \frac{l}{Z/D_{eq} - (Z-l)/D}. \tag{8}$$

If the sample is of double layers, e.g., a CCL deposited on a substrate, the equivalent resistance R_{ceq} may be expressed as

$$R_{ceq} = \frac{Z}{D_{ceq}A} = \frac{Z - l_s - l_c}{DA} + \frac{l_s}{D_{seff}A} + \frac{l_c}{D_{ceff}A}. \tag{9}$$

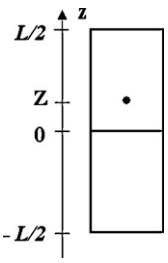

Fig. 1. A schematic diagram of a Loschmidt cell consisting of two chambers: bottom and top. A flat valve was located at $z = 0$. An optic fibre oxygen sensor was poisoned at $z = Z$. The diameter of the oxygen sensor was 300 μm.

Here l_s and l_c are the thickness of the substrate and catalyst layer, respectively. D_{seff} and D_{ceff} are the effective diffusion coefficients of the substrate and catalyst layer, respectively. D_{ceq} is the equivalent diffusion coefficient in the presence of the CCL and the substrate. The effective diffusion coefficient of the catalyst layer D_{ceff} can be found with Eq. (10):

$$D_{ceff} = \frac{l_c}{Z/D_{ceq} - (Z - l_s - l_c)/D - l_s/D_{seff}}, \quad (10)$$

with Eqs. (5), (8) and (10), the effective diffusion coefficient of a porous sample, e.g., a CCL, can be determined.

2.3. CCL sample preparation

The CCL samples contained 30 wt% Nafion ionomer (5 wt% solution, EW1000, Alfa Aeser). The Pt/C catalyst used in this work was 46 wt% Pt/graphitized carbon (Tanaka Kikinzoku Kogyo). The baseline ink formulation contains 1:1 mixture of methanol/water. The mixture was sonicated in a water bath at room temperature for 30 min. Nafion solution was added drop-wise to the mixture. The suspension was homogenized for 60 minutes. The ink was ready to be used for deposition. An automated spray coater (EFD-Ultra TT series) was employed to deposit CCLs onto the Al_2O_3 membrane substrates, Anopore Inorganic Membranes (Anodisc 25, Whatman). Various Pt loadings, 0.2, 0.3, 0.4, 0.6 and 0.8 mg cm^{-2}, corresponding to about 6–29 μm in thickness, were obtained by changing the number of deposition passes. The total of eight CCL samples with different thicknesses were investigated in this work. The porosity and pore size distribution of the catalyst layer were obtained by Hg porosimetry using the same procedure as previously reported [21].

3. Results and discussion

3.1. Substrate

In this work, each CCL sample under investigation was deposited in a piece of substrate. The functional requirements of the substrate are: (1) possessing well-defined pore structure with no/minimum lateral diffusion within the substrate, (2) exhibiting considerably higher diffusion coefficient than that of the catalyst layer such that the limiting transportation is not arising from the substrate, and (3) having pore diameters small enough such that the catalyst layer deposited would not penetrate into the substrate, and thus a well-defined catalyst layer thickness can be determined. In addition, the substrate must be chemically inert to common solvents used during a catalyst layer deposition (e.g., low b.p. alcohols and water).

We found that Al_2O_3 membrane was a good candidate of the substrate satisfying the requirements. The membrane is hydrophilic and compatible with most solvents and aqueous material. According to the vendor, this material has a non-deformable honeycomb pore structure with no lateral crossovers between individual pores. Fig. 2 is an SEM image of the cross section of the membrane "Anodisc 25" from Whatman International Ltd. The image shows how the pore size changes from circa 200 nm on the bottom surface to about 20 nm on the top surface. Table 1 lists the geometrical parameters of the Anodisc 25 quoted from the vendor and measured in this work.

Three Anodisc 25 substrates were measured, and each substrate was measured more than five times. Fig. 3 shows a typical curve

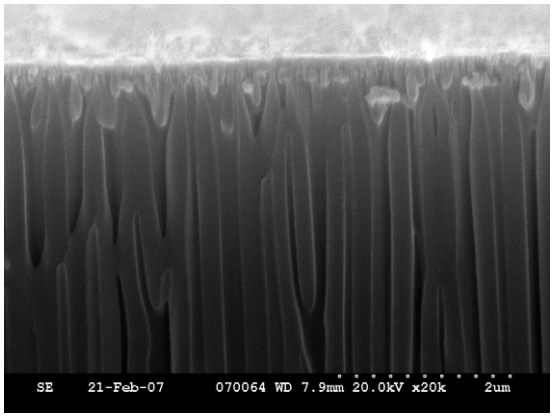

Fig. 2. Cross-section SEM image of the inorganic (Al_3O_2) membrane "Anodisc 25".

of oxygen concentration evolution in the presence of an Anodisc 25 substrate. Fitting Eq. (5) to the concentration curves, we could attain the equivalent diffusion coefficient D_{seq}, and the averaged D_{seq} of the three substrates was $D_{seq} = (1.90 \pm 0.03) \times 10^{-5}$ m^2 s^{-1}. In the experiments, the exact time t_0 of the beginning of the gas diffusion was hard to determine. To find t_0, the t in Eq. (5) was replaced by $t - t_0$ when curve fittings were performed. With Eq. (8), the EGDC D_{seff} of each substrate was calculated, and the arithmetic average of the EGDCs of the three substrates was found to be $D_{seff} = (1.3 \pm 0.3) \times 10^{-6}$ m^2 s^{-1}. In the calculation using Eq. (8), bulk O_2–N_2 diffusion coefficient $D = 2.02 \times 10^{-5}$ m^2 s^{-1} [18] was used.

3.2. Pore size distribution of the CCLs and porosity

The peak pore size and pore size distribution (PSD) of the CCLs were examined by Hg porosimetry, as shown in Fig. 4. In general, the pore size distribution of these CCLs ranges from 10 to 200 nm, which includes meso (2–50 nm diameter) and macro (>50 nm) pores as defined by the International Union of Pure and Applied Chemistry (IUPAC). The peak pore size for these CCLs is about 50 nm. The cumulative intrusion curve represents the integral volume of

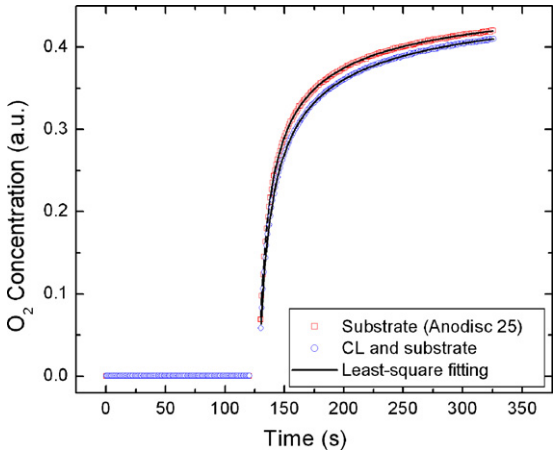

Fig. 3. The oxygen concentration evolution in the top chamber, in the presence of an Anodisc substrate, and a CCL (29 μm) on the top of the substrate, respectively.

Table 1
The geometrical parameters of Anodisc 25 inorganic (Al_2O_3) membranes.

	Average thickness	Diameter with ring	Membrane diameter	Pore size	Porosity
From the vendor	60 μm	25 mm	21 mm	0.02 μm	25–50%
Measured with mercury porosimetry in this work					28%

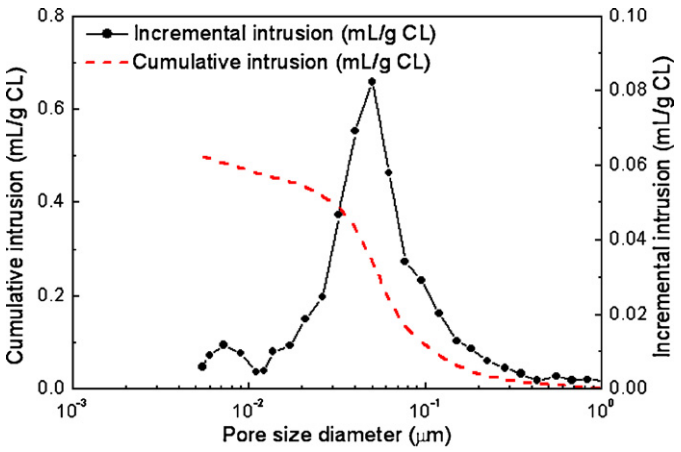

Fig. 4. Typical pore size distribution of the CCLs.

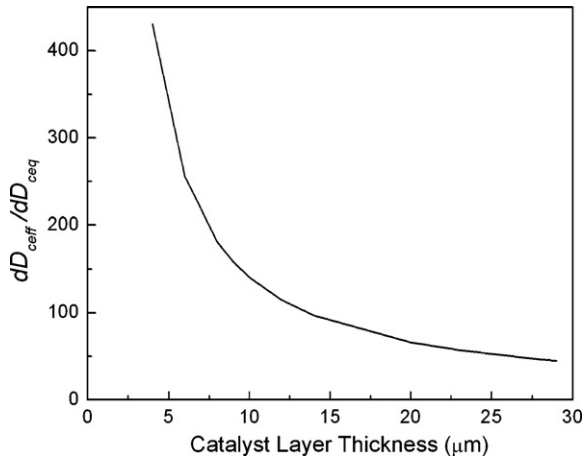

Fig. 5. Numerical simulation of dD_{ceff}/dD_{ceq} using Eq. (10).

Hg penetrated into the pores with diameters ranging from 1 μm to 5 nm. The porosities of the CCLs with different thickness were subsequently calculated to be around 30–40%.

3.3. The effective gas diffusion coefficient of the CCL

The thickness of CCL samples varied from circa 6 μm to about 29 μm, and eight samples of different thicknesses were studied in this work, as shown in Table 2. Each sample was measured more than five times. A typical curve of oxygen concentration evolution in the presence of a CCL and the substrate was shown in Fig. 3. After the determination of the equivalent diffusion coefficient using Eq. (5), the EGDC of each sample could be deduced with Eq. (10). Table 2 exhibits that the D_{ceff} does not change significantly with the thickness of CCLs, and the arithmetic average EGDC of the eight CCLs was found to be $D_{ceff} = (1.5 \pm 0.1) \times 10^{-7}$ m^2 s^{-1}.

It was observed that the EGDC of thin (<10 μm) CCL samples is more sensitive to the fluctuation of D_{ceq} than that of the thick (>10 μm) CCL samples, resulting in a larger deviation of the EGDC of the thin CCL samples. From Eq. (10), one may have

$$\Delta D_{ceff} = \frac{dD_{ceff}}{dD_{ceq}} \Delta D_{ceq}. \tag{11}$$

Fig. 5 reveals that dD_{ceff}/dD_{ceq} increases when the CCL thickness decreases, giving the explanation of the observed phenomenon.

To reduce the influence of the fluctuation on the EGDC, the averaged EGDC could be determined by a least-square curve fitting of the following equation, derived from Eq. (9),

$$D_{ceq} = \frac{Z}{(Z - l_s - l_c)/D + l_s/D_{seff} + l_c/D_{ceff}}, \tag{12}$$

to the experimental data presented in Fig. 6. With the correlation coefficient $R = 0.984$ of the curve fitting, the EGDC thus attained was $D_{ceff} = (1.47 \pm 0.05) \times 10^{-7}$ m^2 s^{-1}, consistent with the foregoing arithmetic average $D_{ceff} = (1.5 \pm 0.1) \times 10^{-7}$ m^2 s^{-1}. Moreover, the EGDC obtained using the curve fitting method has one more significant digit than the arithmetic average, improving the measurement precision.

Table 2
Measured equivalent and effective binary gas diffusion coefficients of catalyst layers.

l_c (μm)	D_{ceq} (10^{-5} m^2 s^{-1})	D_{ceff} (10^{-7} m^2 s^{-1})
6	1.81 ± 0.03	1.36
9	1.81 ± 0.04	1.67
10	1.73 ± 0.04	1.24
12	1.75 ± 0.02	1.50
14	1.72 ± 0.02	1.47
20	1.67 ± 0.03	1.62
23	1.62 ± 0.03	1.50
29	1.54 ± 0.01	1.43

In Eqs. (9), (10) and (12) the possible diffusion resistance of the interface between the substrate and the CCL on the top of the substrate is not taken into account. To find the possible diffusion resistance, we rewrite Eq. (9) as

$$R_{ceq}A = \frac{Z}{D_{ceq}} = \frac{Z - l_s - l_c}{D} + \frac{l_s}{D_{seff}} + \frac{l_c}{D_{ceff}} = \left(\frac{1}{D_{ceff}} - \frac{1}{D}\right) l_c + \left(\frac{Z - l_s}{D} + \frac{l_s}{D_{seff}}\right) = \left(\frac{1}{D_{ceff}} - \frac{1}{D}\right) l_c + \frac{Z}{D_{seq}}. \tag{13}$$

Eq. (13) exhibits that $R_{ceq}A$ is a linear function of the CCL thickness l_c; the slope of $R_{ceq}A$ is basically decided by D_{ceff}, and the intercept should be Z/D_{seq} if there is no diffusion resistance at the interface. Fig. 7 presents a least-square linear fitting to the expermental data of Z/D_{ceq}. For a linear fitting there exists a best approximation [22]. The intercept of the linear fitting was found to be 8.33×10^3 m^{-1} s. With $D_{seq} = (1.90 \pm 0.03) \times 10^{-5}$ m^2 s^{-1}, Z/D_{seq} is in the range of $8.26–8.53 \times 10^3$ m^{-1} s. The intercept found is within the range, indicating that the diffusion resistance of the interface is negligible.

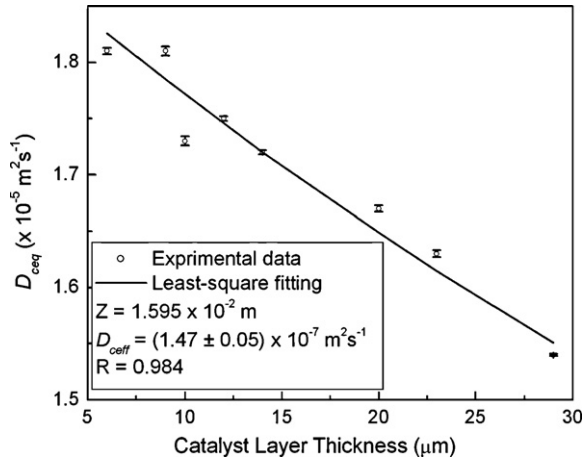

Fig. 6. Experimental data of the equivalent diffusion coefficients of the eight CCLs of different thicknesses and the least-square curve fitting Eq. (12) to the experimental data: $Z = 1.595 \times 10^{-2}$ m, $D_{seff} = (1.3 \pm 0.3) \times 10^{-6}$ m^2 s^{-1}, and $l_s = 6.0 \times 10^{-5}$ m were used in the fitting. The correlation coefficient between the fitting and the experimental data $R = 0.984$ was found.

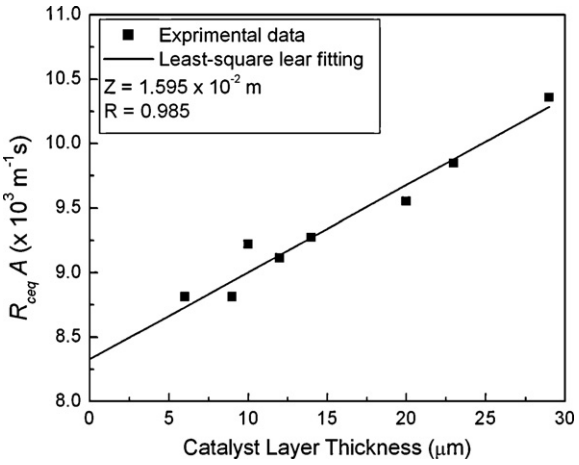

Fig. 7. A best linear fitting to the expermental data of $R_{ceq}A$ (i.e., Z/D_{ceq}).

3.4. The Knudsen effect

The Bridgeman formula, $D_{ceff} = D\varepsilon^{1.5}$, has been widely used for calculating the EGDC of catalyst layers of PEM fuel cells. Here ε is porosity. Through these experimental measurements of the 8 CCL samples, we found that Bruggeman's formula overestimates the EGDC of the CCL samples. The porosity of the eight samples ranges from 30 to 40%, so the average EGDC of the 8 samples, calculated based on $D_{ceff} = D\varepsilon^{1.5}$, is about $D_{ceff} = 2.02 \times 10^{-5}(0.35)^{1.5} = 4.18 \times 10^{-6}$ m^2 s^{-1}. Comparing with the measured EGDC of the CCL samples, $D_{ceff} = (1.5 \pm 0.1) \times 10^{-7}$ m^2 s^{-1}, the EGDC of the CCLs from Bruggeman's formula is one order higher than the measured one. This considerable difference is due to the fact that Bruggeman's formula, $D_{ceff} = D\varepsilon^{1.5}$, fails to take into account the Knudsen effect. Generally speaking, the Knudsen effect is not negligible when pore size is as small as one micrometer, and becomes dominant when pore size is less than 100 nm. As can be seen from Fig. 4, the pore size distribution of the CCL samples ranges from 10 to 200 nm with the peak pore size around 50 nm, meaning that the Knudsen effect has to be considered.

Mu et al. [2] proposed a method for calculating the EGDC with the Knudsen effect included using a finite element method. In Mu's method [2], the entire pore space in a porous layer is discretized into a number of small tubes with different diameters. The porosity, the average diameter and the standard deviation of diameters of the small tubes can be specified. In a single cylindrical pore, the effective diffusion coefficient, D_{eff}, is represented by, $1/D_{eff} = 1/D_b + 1/D_k$, where D_b is the bulk diffusion coefficient, and D_k is the Knudsen diffusion coefficient, which is given by $D_k = 48.5 d_p \sqrt{T/M}$. Here d_p is pore diameter, T is temperature and M is molecular weight. Mu's results show that when the Knudsen effect is counted, the effective gas diffusion coefficient of the catalyst layer with mean pore size 50 nm and porosity 40%, is about 15% of the effective gas diffusion coefficient without the Knudsen effect included. This is basically in agreement with the effective gas diffusion coefficients measured experimentally in this paper.

4. Conclusions

An in-house made Loschmidt diffusion cell was employeed to measure the effective coefficient of binary gas diffusion through cathode catalyst layers of PEM fuel cells. Each CCL under investigation was deposited on a substrate of Al_2O_3 membrane, and the thicknesses of the eight CCLs varied from 6 to 29 μm. With the diffusion signal processing procedure developed in this work, we found that the EGDC of the substrate was one order higher than that of the CCLs, exhibiting that the binary gas diffusion through the CCL-substrate assembly was dominated by the CCL. Also, the diffusion resistance of the interface between the CCL and the substrate did not play a significant role in the diffusion. The EGDC of the CCLs was found to be $(1.47 \pm 0.05) \times 10^{-7}$ m^2 s^{-1}, which is much smaller than that predicted by Bruggeman's formula. Our analysis shows that the binary gas diffusion through the CCLs is dominated by the Knudsen effect.

Acknowledgements

The support from the Technology Development Program on Proton Exchange Membrane Fuel Cell (TDP-PEMFC) of National Research Council and its industrial collaborators, Ballard Power Systems and Automotive Fuel Cell Cooperation, is appreciated.

References

[1] Q. Wang, M. Eikerling, D. Song, Z. Liu, T. Navessin, Z. Xie, S. Holdcroft, J. Electrochem. Soc. 151 (2004) A950.
[2] D. Mu, Z.S. Liu, C. Huang, N. Djilali, Microfluid. Nanofluid. 4 (2008) 257.
[3] N. Zamel, X. Li, J. Shen, Energy Fuels 23 (2009) 6070.
[4] D.A.G. Bruggeman, Annalen der Physik (Leipzin) 24 (1935) 636.
[5] P.K. Das, Z. Li, Z.S. Liu, Appl. Energy 87 (2010) 2785.
[6] D. Mu, Z. Liu, C. Huang, N. Djilali, J. Porous Mater. 14 (2007) 49.
[7] J.H Nam, M. Kaviany, Int. J. Heat Mass Transfer 46 (2003) 4595.
[8] A.Z. Weber, J. Newman, Chem. Rev. 104 (2004) 4679.
[9] F. Zhang, R.E. Hayes, S.T. Kolaczwski, Trans. Inst. Chem. Eng. A 82 (2004) 481.
[10] I.S. Park, D.D. Do, Catal. Rev. Sci. Eng. 38 (1996) 189.
[11] N. Zamel, X. Li, N.G. Astrath, J. Shen, J. Zhou, F.B. Astrath, H. Wang, Z.S. Liu, Chem. Eng. Sci. 65 (2010) 931.
[12] P.T. Callaghan, Principles of Nuclear Magnetic Resonance Microscopy, Oxford University Press, New York, 1994.
[13] P.D. Majors, D.M. Smith, P.J. Davis, Chem. Eng. Sci. 46 (1991) 3037.
[14] D. Kramer, S.A. Freunberger, R. Flückiger, R. Schneider, I.A. Wokaun, F.N. Büchi, G.G. Scherer, J. Electroanal. Chem. 612 (2008) 63.
[15] R. Flückiger, S.A. Freunberger, D. Kramer, A. Wokaun, G.G. Scherer, F.N. Büchi, Electrochim. Acta 54 (2008) 551.
[16] J. Baranski, E. Bich, E. Vogel, J.K. Lehmann, Int. J. Thermophys. 24 (2003) 1207.
[17] J.R. Rohling, J. Shen, C. Wang, J. Zhou, C.E. Gu, Appl. Phys. B 87 (2007) 355.
[18] N.G.C. Astrath, J. Shen, D. Song, J.H. Rohling, F.B.G. Astrath, J. Zhou, T. Navessin, Z.S. Liu, C.E. Gu, X. Zhao, J. Phys. Chem. 113 (2009) 8369.
[19] N.G.C. Astrath, J. Shen, F.B.G. Astrath, J. Zhou, C. Huang, X. Yuan, H. Wang, T. Navessin, Z.S. Liu, G. Vlajnic, D. Bessarabov, X. Zhao, Rev. Sci. Instrum. 81 (2010) 046104.
[20] J. Crank, The Mathematics of Diffusion, second ed., Oxford University Press, New York, 1975.
[21] Z. Xie, X. Zhao, M. Adachi, Z. Shi, T. Mashio, A. Ohma, K. Shinohara, S. Holdcroft, T. Navessin, Energy Envinron. Sci. 1 (2008) 184.
[22] G. Meinardus, Approximation of Functions: Theory and Numerical Methods, Springer-Verlag, Berlin, 1967 [Chapter 1].